

CFD-Based, Lagrangian-Eulerian coupling approach for Magnetophoretic Particle Capture

Saud A. KHASHAN^{1*}, Edward FURLANI^{2,3}

* Corresponding author: Fax: +9713-7623158; Email: skhashan@uaeu.ac.ae

1: Mechanical Engineering Department, United Arab Emirates University, UAE

2: Dept. of Chemical and Biological Engineering

3: Dept. of Electrical Engineering, University at Buffalo, SUNY, efurlani@buffalo.edu,

Abstract We study magnetophoretic capture of magnetic particles in microfluidic devices and present a parametric characterization for the capture efficiency. We model particle transport and capture using a computational fluid dynamic, CFD-based, Lagrangian-Eulerian approach that takes into account the dominant particle forces and particle-fluid coupling. We introduced two dimensionless groups that characterize particle capture, one that scales the magnetic and hydrodynamic forces on the particle and another that scales the distance to the magnetic field source. We use the model to parameterize capture efficiency with respect to the dimensionless numbers for both one-way and two-way particle-fluid coupling. We demonstrate that for dilute suspensions, the simplified one-way coupling analysis marginally under-predicts the capture efficiency computed using the two-way fully coupled analysis.

Keywords: Magnetophoresis, magnetic particles, microfluidic devices, MEMS

1. Introduction

Over the last several years the interest in Magnetophoretic Particle Capture in Microfluidic Systems has grown dramatically, especially for applications in fields such as microbiology and biotechnology (Furlani 2010a; Furlani 2010b; Ganguly 2010; Gijs 2004). Magnetic particles can be functionalized to selectively bind to target biomaterials such as proteins, enzymes, nucleic acids or whole cells thereby enabling magnetophoretic control of these materials (Pankhurst et al. 2009; Berry 2009; Arrueboa et al. 2007; Majewski and Thierry 2007; Safarik and Safarikova 2002). This capability is being leveraged through advances in microfluidics that enable miniature biochemical laboratories to be integrated into a single microsystem, i.e. Lab-on-a-chip and “micro total analysis systems” (μ TAS). Such microsystems typically range in size from millimeters to the centimeters and are usually made using planar glass-, silicon- or polymer-based substrates. Fluidic structures within these systems such as mixing chambers and

flow channels range from several to hundreds of microns in size. Magnetic functionality can be integrated into these systems by embedding magnetic field source elements in the substrate, in proximity to the flow channels. These elements can be magnetically passive structures such as nickel-based microbars, or active voltage-driven conductors (Choi et. al. 2001; Furlani 2001; Smistrup et. al. 2005; Furlani 2006; Furlani and Sahoo 2006; Furlani et al. 2007; Smistrup et. al. 2008). In the former case, an external field source is used to magnetize the elements. In the latter case, circuitry is required to activate the conductors. In either case, the source elements generate a magnetic field distribution that gives rise to a magnetic force on magnetically labeled material as it flows through a microchannel, thereby enabling magnetophoretic control to sort or immobilize the material.

Continuous flow separation enables a relatively high throughput of a sample and it allows for real-time monitoring of separation efficiency. The latter capability enables on-line feedback for optimization, which can be

achieved by adjusting parameters such as the flow rate and the induced force. In addition, the continuous flow approach can accommodate multiple inlets and outlets for the simultaneous separation of multiple sample components. The continuous nature of the separation process lends itself to a high level of integration with other upstream or downstream process. Various mechanisms have been used to fractionate sample components in continuous flow applications including electric forces, standing ultrasonic waves and arrangements of obstacles in the flow path. Magnetic separation has also been successfully used for this process. An early commercialized magnetic cell separation system that utilized permanent magnets to generate the magnetic force was employed to separate cells labeled with biotinylated superparamagnetic ferrit-dextran beads (Miltonic et al. 1990). Other systems using micromagnetic elements have been used for the complete separation of 1 μ m magnetic particles (Smistrup et al. 2006).

In this paper, we develop a scaled fully-coupled particle-fluid model for predicting the transport and capture of magnetic particles in microfluidic systems. The model involves a CFD-based Eulerian-Lagrangian analysis that includes the dominant forces on the particles and two-way momentum transfer between the moving particles and the flow field. To our knowledge, this is one of the first studies of particle separation in microfluidic system that is based on fully-coupled particle-fluid CFD analysis. Our model takes into account key magnetic variables including the size and magnetic properties of the particles and the magnetic field parameters, i.e. the magnitude and gradient of the field as well as the distance of the field source to the microchannel. It also accounts for fluidic parameters including the dimensions of the microchannel and the fluid viscosity. Several simplifying assumptions are made in the analysis. Specifically, we assume the fluid is incompressible and that the flow is laminar, which is usually the case in microfluidic devices. We further assume that the particle suspension is sufficiently dilute so

that particle-particle interactions can be neglected. Particle coagulation as well as build-up and subsequent channel blockage are also neglected. The particle magnetism is assumed to be in the linear range, below saturation. We also assume that the particles enter the channel with a uniform spatial distribution.

In the development of the model we introduce two dimensionless groups that characterize particle capture, one that scales the magnetic and hydrodynamic forces on the particle and another that scales the distance to the magnetic field source. We use the model to parameterize capture efficiency with respect to the dimensionless numbers for both one-way and two-way particle-fluid coupling. For one-way coupling in which the particle motion does not alter the flow momentum, we develop correlations that provide insight into system performance towards optimization. We quantify for the first time the difference in capture efficiency predicted using one-way versus two-way coupling analysis. Our work demonstrates that one-way coupling provides a conservative estimate of capture efficiency. Specifically, it over predicts the magnetic force needed for particle capture compared to the more rigorous fully-coupled analysis. As such, one-way coupling can be used for rapid parametric screening of particle capture performance. However, more accurate predictions require two-way particle-fluid coupling analysis. This is especially true when considering higher capture efficiencies and/or higher particle concentrations.

2. Mathematical Formulation

Broadly speaking, two approaches are commonly used to model particle transport in microfluidic systems, the Eulerian and the Lagrangian approaches. In the Eulerian approach particles are modeled collectively in terms of a time-dependent spatially-varying concentration. The concentration is governed by a PDE that accounts for both force-induced drift and Brownian diffusivity of the particles (Khashan et al. 2011; Furlani and Ng 2008).

The Eulerian method is used to study the behavior of sub-micron particles when the Brownian diffusivity, as modeled by a Stokes-Einstein-like equation, has a significant impact on the particle transport. In this case, the particles are assumed to respond instantaneously (with a negligibly short acceleration) to a balance between the fluidic drag and magnetic forces. The particle moves at a constant terminal velocity relative to the base fluid, which is commonly referred to as the magnetophoretic velocity. This velocity adds to fluid velocity to define the overall particle motion that drives its convective flux in the Eulerian frame work. The PDE that governs the particle concentration has the same form as the fluidic momentum equations and can be solved simultaneously with these equations using almost the same numeric algorithm. Thus, an Eulerian-based particle transport model can be readily integrated into Eulerian-based CFD codes (Khashan et al. 2011; Khashan and Haik 2006).

In the Lagrangian approach, particles are treated as discrete entities and the trajectory of each particle is determined by integrating the Newtonian equations of motion. The fluid is governed by the Navier-Stokes equations and the flow field is usually considered to be incompressible. This approach is appropriate for larger particles when Brownian motion is negligible.

In this paper we use a combined Lagrangian-Eulerian CFD-based approach to model the fully-coupled particle-fluid behavior of magnetic particles in a microfluidic channel under the influence of a magnetic force. We use a Lagrangian analysis to track the motion of individual particles, and we couple the particle motion to the fluid by introducing a particle force sink into the Navier Stokes momentum equations, which are solved using an Eulerian-based CFD analysis. The application of two-way coupling is a key result of this work and distinguishes it from most other studies that consider only one-way particle-fluid coupling. We quantify for the first time the difference in capture efficiency

predicted using one-way versus two-way coupling analysis as described below.

The magnetic force as applied on the magnetic particle suspended in a state of dilute suspension in a non-conducting carrier fluid can be expressed as (Furlani EP 2010c)

$$\vec{F}_{mag} = \frac{1}{2} \mu_o \chi_m V_p \nabla H^2 \quad (1)$$

where μ_o is the free-space magnetic permeability and χ_m (dimensionless) is the effective volume-averaged susceptibility of the linearly magnetic particle, which is estimated based on its magnetically active volume and relative to the susceptibility of the carrier fluid, i.e. the magnetic moments of the polymeric-based microparticles are derived completely from the magnetic nanocrystals encapsulated or embedded in the polymer matrix . Here $H = (\vec{H} \cdot \vec{H})^{1/2}$ is the magnitude of the applied external magnetic field (A/m), which can be related to the magnetic field induction \vec{B} (in T) of a particle suspended in a non-magnetic or weakly diamagnetic fluid by $\vec{B} = \vec{H} / \mu_o$. Both \vec{H} and \vec{B} can be determined from Maxwell's field equations under magneto-static conditions. With the particle's mobility defined as $(3\pi\eta d_p)^{-1}$ the adopted particle motion takes the form:

$$m_p \frac{d\vec{u}_p}{dx} = b^{-1} (\vec{u} - \vec{u}_p) + V_p (\rho_p - \rho) \vec{g} + \frac{1}{2} \mu_o \chi_m V_p \nabla H^2 \quad (2)$$

The variables \vec{u} , ρ and η are the instantaneous local velocity vector, density and the molecular viscosity, respectively, of the carrier fluid ρ_p , a and V_p are the density, radius and volume of the particle, and \vec{g} is the gravitational acceleration. The trajectory equations are solved by stepwise integration over discrete time steps. Integration of time in particle motion equation yields the velocity of the particle at each point along the trajectory as

$$\frac{d\vec{u}_p}{dx} = \tau^{-1} (\vec{u} - \vec{u}_p) + \vec{a} \quad (3)$$

where

$$\vec{a} = \frac{V_p(\rho_p - \rho)\vec{g} + \frac{1}{2}\mu_o\chi_m V_p \nabla H^2}{m_p} \quad (4)$$

and $\tau = m_p b$. The trajectory can be predicted using

$$\frac{d\vec{x}}{dt} = \vec{u}_p \quad (5)$$

Here τ presents the time required for a particle to respond to changes in the base fluid motion, also, referred to as the particle relaxation time. Note that Eqs. (3) and (5) are a set of coupled ordinary differential equations. These can be integrated using a number of different numerical techniques. We have used a fourth-order Runge-Kutta method for our analysis (Furlani and Sahoo 2006).

We model the fluid phase using a Eulerian approach. The fluid velocity field is described by the Eulerian incompressible Navier-Stokes equations

$$\nabla \cdot \vec{u} = 0 \quad (6)$$

$$\rho \left(\frac{\partial \vec{u}}{\partial t} + \vec{u} \nabla \vec{u} \right) = -\nabla P + \nabla \cdot (\eta \nabla \vec{u}) \quad (7)$$

$$-\frac{1}{V_{cell}} \sum_{j=1}^{N_{p,cell}} \vec{f}_{ff}$$

In this study, the particle volume fraction is sufficiently low so that its effect on the continuity equation and on the inertia and stress flux terms of the momentum equation is neglected. The two-way coupling is accounted for through the last sink term that accounts for the drag, buoyancy and magnetic forces (the right-hand side of the Lagrangian equation) for all particles in each fluidic computational cell, where V_{cell} is the volume of a computational cell, $N_{p,cell}$ is the number of particles in that cell and \vec{f}_{ff} is the fluid force on the j 'th particle in that cell. In other words, force \vec{f}_{ff} simulates the interphase momentum transfer from the continuous fluid to a single j 'th particle. This force is equal but opposite to the force that a particle exerts on the fluid ($-\vec{f}_{ff}$), which is thus the sink term for continuous-phase equation. It is important to

note that for this approach to work, the particle size should be much smaller than the size of the cells that make up the fluidic computational domain.

3 Flow-Magnetic Configurations

We apply the model described above to the analysis of particle transport and capture in a Newtonian fluid flowing in a two-dimensional microchannel as shown in Figure 1. We perform a parametric analysis of this system about a base configuration in which the microchannel has a height $h = 100 \mu m$ and a length $L = 1000 \mu m$. A magnetic dipole field source in the form of a pair of anti-parallel current carrying conductors is positioned at a distance $y_{mag} = 100 \mu m$ beneath the lower wall of the microchannel, midway along its length ($x_{mag} = 500 \mu m$).

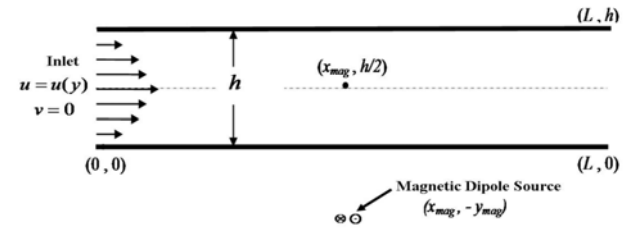


Figure 1: Microfluidic System with magnetic dipole source.

In the following analysis the width of the channel (into the page) is assumed to be sufficiently large to justify a two-dimensional flow analysis, i.e. we ignore flow variation in that direction. The channel height is large enough to justify a continuum Newtonian fluid analysis and we ignore particle-wall hydrodynamic interactions. The length of the channel is sufficiently long so that hydrodynamic effects at the inlet and outlet do not impact the magnetic field-directed particle motion near the mid-length of the channel.

In our model, incompressible fluid enters the channel at the left side (inlet) with a fully developed laminar flow profile in which the average velocity is $u_i = 200 \mu m/s$. The outlet pressure is set to zero. Solid spherical magnetic particles are injected into the

computational domain at the inlet with a uniform distribution over the entrance plane. We assume that the fluid is water, which is essentially nonmagnetic. The viscosity and density are $\eta = 0.001 \text{ Ns/m}^2$ and $\rho_f = 1000 \text{ kg/m}^3$, respectively. The properties of the magnetic particles are chosen to be compatible with the MyOne™ beads (www.dynabead.com). The particle has a radius $a = 0.525 \text{ } \mu\text{m}$, density $\rho_p = 1700 \text{ kg/m}^3$, saturation magnetization $M_s = 4.3 \times 10^4 \text{ A/m}$ and an “effective” susceptibility $\chi = 1.4$. The magnetization of the particles will be below saturation as long as $B \leq \mu_0 M_s / \chi$ where $B = |\mathbf{B}|$ (Furlani et al. 2007). This will occur as long as B does not exceed 38 mT, which was the case in all simulations. The particle volume fraction for our base analysis is 2%. It is important to note that the particle size is much smaller than the grid size in the computational domain so that many particles can exist within a computational cell. This condition is needed when computing the momentum transfer from the particles to the fluid. Lastly, the channel walls are assumed to be nonmagnetic and therefore are treated as boundaries in the simulation model.

3 Results and Analysis

The performance criterion for magnetic separation is defined in terms of collection efficiency, which is the percentage of incoming particles that are captured (trapped) in the microchannel by the magnetic force. First, we sought a dimensionless group that scales both the magnetic and drag force on the particles. Accordingly, we present the following two dimensionless groups

$$\beta = \frac{1}{2} \mu_0 \chi V_p p^2 / (6\pi\eta a u_i h^5) \quad (8)$$

and

$$\gamma = y_{mag} / h. \quad (9)$$

where $p = Id / 2\pi$, I is the current in each conductor and d is the distance between the conductors. It should be noted that β is

independent of the location of the magnetic source, while γ depends on the position of the source and therefore the field gradient that it generates within the microchannel. Note that scaling the magnetic and fluidic forces with β directly accounts for the increased magnetic force due to larger effective particle susceptibility and size. It also accounts for the particle’s mobility, defined as $(6\pi\eta a)^{-1}$, in different viscous base fluids.

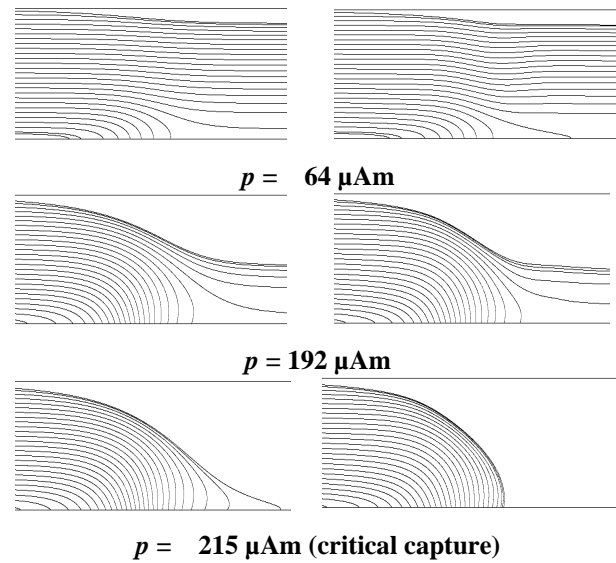


Figure 2: Comparison of predicted particle trajectories using one-way coupling (left) and two-way coupling (right) for the base problem ($h=100 \text{ } \mu\text{m}$, $L=1000 \text{ } \mu\text{m}$, $y_c = y_{mag}=100 \text{ } \mu\text{m}$, $x_{mag}=500 \text{ } \mu\text{m}$, $u_i=200 \text{ } \mu\text{m/s}$, $d_p = 1.05 \text{ } \mu\text{m}$, $\chi = 1.4$, and $\eta = 10^{-3} \text{ N.s/m}^2$). The trajectories (sampled over a selected section of the microchannel) show an increased particle capture efficiency with increased dipole field strength.

From this figure, we find that the one-way coupling analysis under-predicts particle capture relative to the two-way fully-coupled analysis. That is, the magnetic force required to achieve a given capture efficiency is predicted to be higher using one-way coupling as compared to the fully-coupled analysis. The $p=215 \text{ } \mu\text{Am}$ calculations are illustrative of this effect. Specifically, for one-way coupling, this field strength renders critical particle capture, i.e. all particles are captured, albeit some at locations beyond the dipole field source. However, it is obvious that the critical particle capture occurs for a lower field strength (i.e.

for p between $192 \mu\text{Am}$ $215 \mu\text{Am}$) in the two-way coupling analysis. One reason for this is that two-way coupled particles act to decrease the fluid velocity in proximity to the magnet, which in turn promotes particle capture in this region. Two-way coupled particles in effect increase the bulk effective viscosity of the fluid, whereas one-way coupled particles have no impact on the momentum or viscosity or fluid flow.

Next, we study the capture efficiency CE as a function of the dimensionless number β , where

$$CE = \frac{\text{number of particles captured}}{\text{total number of particles}} \quad (10)$$

Figure 3 shows the capture efficiency CE vs. β with γ fixed ($\gamma=1$) for one-way coupling. Note that a single curve is obtained for all variations of the inlet velocity, particle diameter, particle magnetic susceptibility and fluid viscosity as long as γ is held constant.

In our study, particles are assumed to be captured once they contact the lower plate (at $y = y_{mag}$). In many cases, they are captured at locations well before the outlet as shown in Fig. 2 c, and it might be more appropriate to define capture efficiency with respect to a desired target site rather than the whole length of the lower wall. This is especially the case when confined particle focusing or separation is desired. The $CE - \beta$ correspondence at fixed γ is also illustrated in Fig. 3 for different values of the hydraulic channel diameter h . It is evident from the figure that the unique correspondence holds even though the inlet mass flow rate of the base fluid ($\sim u_i h$) is doubled for each γ cases.

Figure 4 below shows two distinct $CE - \beta$ relations for γ equal to 1.0 and 0.5, respectively. These plots indicate that at smaller γ (i.e. the magnetic source closer to the microchannel), a higher capture efficiency can be obtained at smaller β . For instance, at $\beta = 0.25$, the capture efficiency is about 40% and 80%, for $\gamma=1$ and 0.5, respectively.

Figure 5 presents the critical $\beta_{cr} - \gamma$ correspondence at which complete capture $CE=1$ can be achieved under the assumption of one-way coupling. A lower particle magnetization is needed when the magnetic source is brought closer to the microchannel, a condition that obviously corresponds to a higher gradient and, therefore, a higher magnetic force. Over the considered γ range, the critical β_{cr} can be expressed in the following analytical form

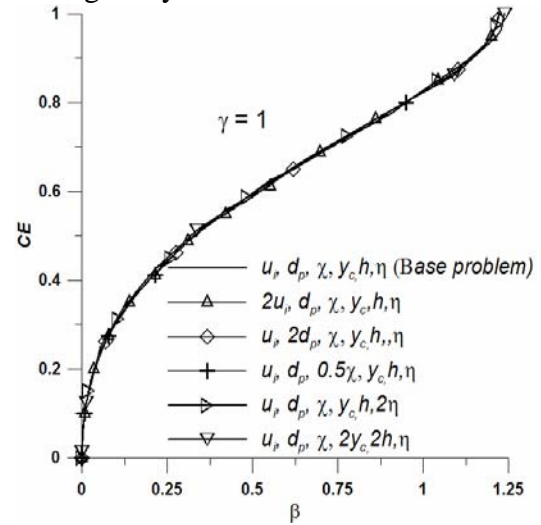


Figure 3: The capture efficiency CE versus β at $\gamma=1.0$ (one-way coupling analysis). The base problem corresponds to $h=100 \mu\text{m}$, $L=1000 \mu\text{m}$, $y_c = y_{mag}=100 \mu\text{m}$, $x_{mag}=500 \mu\text{m}$, $u_i=200 \mu\text{m/s}$, $d_p = 1.05 \mu\text{m}$, $\chi = 1.4$, and $\eta = 10^{-3} \text{ N.s/m}^2$.

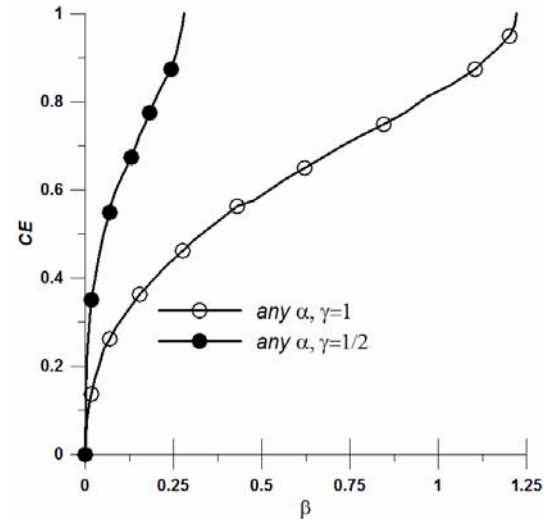


Figure 4: The capture efficiency CE versus β at $\gamma=1.0$ and 0.5 (one-way coupling analysis). The parameter α , as defined by equation 20 can be any value.

$$\beta_{cr} = \frac{\alpha p_{cr}^2}{h^5} \approx 1.14\gamma^3 - 0.41\gamma^2 + 0.5\gamma. \quad (11)$$

This equation provides a direct means to relate the following parameters: α (a grouping of hydrodynamics and magnetization parameters), h (the microchannel height) and P_{cr} (the required critical dipole strength) to the parameter γ . Thus, we can use this expression to correlate the critical β and γ values at which we have complete capture. Furthermore, the definition of β indicates that this equation may be used to relate a variation in any of α , p_{cr} or h with respect to γ at complete capture. Another important point is that this correlation, which is based on one-way coupling, can be used as a conservative design parameter for the more rigorous two-way coupling.

Figure 6 shows a comparison of the predicted capture efficiency using one-way versus a two-way coupling analysis for two different values of γ . Note that for both values of γ the one-way and two-way coupled simulations yield approximately the same functional profile for values of β that render $CE \leq 0.6$. However, the former under predicts the latter for larger values of β . This last result is important, and is a key finding of this study. Specifically, we quantify for the first time the difference in capture efficiency predicted using one-way versus two-way coupling analysis. Specifically, we show that one-way coupling over predicts the magnetic force needed for particle capture as compared to the more rigorous fully-coupled analysis, especially at higher capture efficiencies and/or higher particle concentrations.

4 Conclusion

There are many advantages to using magnetic-based biomanipulation and it has been successfully implemented in microfluidic devices for applications that include bioseparation and continuous cell sorting. However, despite the versatility and potential impact of this approach, the development of rigorous transport models that account for fully-coupled particle-fluid interactions are

lacking. In this paper, we have presented a model for predicting field-directed transport of colloidal magnetic particles in microfluidic systems taking into account two-way particle-fluid coupling. The method involves the use a CFD-based Lagrangian-Eulerian approach to predict the transport and capture of particles and the impact of their motion on the flow field. We have demonstrated the method via application to particle transport and capture in a two-dimensional laminar flow field within a microfluidic channel. The magnetic force on the particles is generated by a dipole field source, which is in the form of two anti-parallel current carrying wires located beneath the channel and midway along its length. We have introduced two dimensionless groups for this analysis that characterize particle capture.

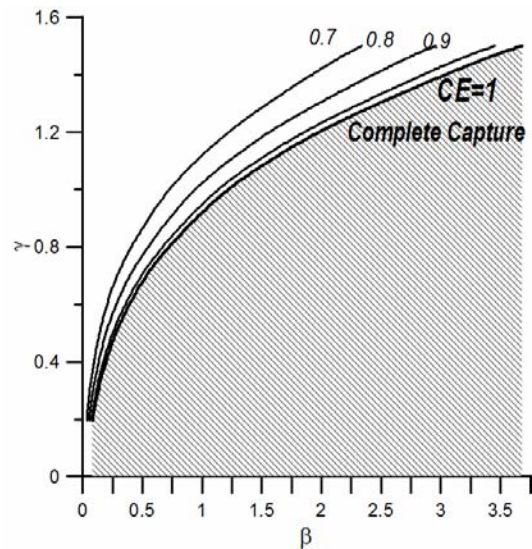


Figure 5: CE map with respect to γ and β (one-way coupling analysis). The shaded area below $CE=1.0$ corresponds to complete particle capture.

One group scales the magnetic and hydrodynamic forces on the particle and the other scales the distance to the magnetic field source. We show that one-way coupling over predicts the magnetic force needed for particle capture as compared to two-way coupling analysis. As such, it can be used for rapid parametric screening of novel magnetic particle capture systems.

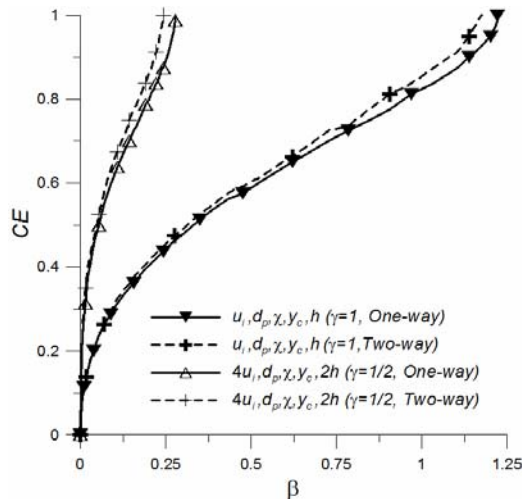


Figure 6: The capture efficiency CE versus β at $\gamma=1.0$ (one-way coupling analysis). The base problem corresponds to $h=100 \mu\text{m}$, $L=1000 \mu\text{m}$, $y_c = y_{\text{mag}}=100 \mu\text{m}$, $x_{\text{mag}}=500 \mu\text{m}$, $u_i=200 \mu\text{m/s}$, $d_p=1.05 \mu\text{m}$, $\chi=1.4$, and $\eta=10^{-3} \text{ N.s/m}^2$.

ACKNOWLEDGEMENT

The first author acknowledges the financial support received from the Research Affairs at the UAE University under contract number. 01-05-7-12/10.

References

- Arrueboa, M., Fernández-Pacheco, R., Ibarra, R.M. et al., 2007, Magnetic nanoparticles for drug delivery. *Nanotoday* 2(3), 22-32.
- Berry, C. C., 2009, Progress in functionalization of magnetic nanoparticles for applications in biomedicine. *J. Phys. D: Appl. Phys.* 42, 224003 (9pp).
- Choi, J-W., Liakopoulos, T. M. and Ahn, C. H., 2001, An on-chip magnetic bead separator using spiral electromagnets with semi-encapsulated permalloy. *Biosensors & Bioelectronics*. 16, 409-416.
- Furlani, E. P., 2010a, Magnetic Biotransport: Analysis and Applications. *Materials*, 3(4), 2412-2446.
- Furlani, E. P., 2010b, Particle Transport in Magnetophoretic Microsystems. In: Kumar C. S. S. R. (ed), *Microfluidic Devices in Nanotechnology: Fundamental Concepts*, John Wiley, NY, pp: 215-262.
- Furlani, E. P., 2010c, Nanoscale Magnetic Biotransport. In: Sattler K (ed) *Handbook of Nanophysics*, CRC Press.
- Furlani, E. P., 2006, Analysis of Particle Transport in a Magnetophoretic Microsystem. *J. Appl. Phys.* 99 (2), 024912 (11pp).
- Furlani, E. P., 2001, Permanent Magnet and Electromechanical Devices; *Materials, Analysis and Applications*. Academic Press, NY.
- Furlani, E. P., and Ng, K. C., 2008, Nanoscale magnetic biotransport with application to magnetofection. *Phys. Rev. E* 77, 061914 (8 pages).

- Furlani, E. P., and Sahoo, Y., 2006, Analytical model for the magnetic field and force in a magnetophoretic microsystem. *J. Phys. D - Appl. Phys.* 39, 1724-1732
- Furlani, E. P., Sahoo, Y., Ng, K. C., Wortman, J. C., and Monk, T. E., 2007, A model for predicting magnetic particle capture in a microfluidic bioseparator. *Biomedical Microdevices* 9 (4), 451-463
- Ganguly, R., and Puri, I. K., 2010, *Microfluidic transport in magnetic MEMS and bioMEMS*. Wiley Interdisciplinary Reviews: Nanomedicine and Nanobiotechnology 2(4), 382-399
- Gijs, M. A. M., 2004, Magnetic bead handling on-chip: new opportunities for analytical applications. *Microfluidics and Nanofluidics* 1 (1), 22-40.
- Khashan, S. A., Elnajjar, E., and Haik, Y., 2011, Numerical Simulation of the Continuous Biomagnetic Separation in a Two-dimensional Channel, *International Journal of Multiphase Flow*, In-press.
- Khashan, S. A., and Haik, Y., 2006, Numerical Simulation of Bio-magnetic Fluid Downstream an Eccentric Stenotic Orifice, *Physics of Fluids*. 18 (11), 113601.
- Majewski, P., and Thierry, B., 2007, Functionalized magnetite nanoparticles - synthesis, properties, and bio-Applications. *Critical Reviews in Solid State and Materials Sciences* 32, 203-215.
- Miltenyi, S., Muller, W., Weichel, W., Radbruch, A., 1990, High gradient magnetic cell separation with MACS. *Cytometry* 11, 231-238.
- Pankhurst, Q. A., Thanh, N. K. T., Jones, S. K., and Dobson, J., 2009, Progress in applications of magnetic nanoparticles in biomedicine. *J. Phys. D: Appl. Phys* 42, 224001.
- Safarik, I., and Safarikova, M., 2002, Magnetic nanoparticles and biosciences. *Monatshefte fur Chemie* 133, 737-759.
- Smistrup, K., Hansen, O., Bruus, H., and Hansen, M. F., 2005, Magnetic separation in microfluidic systems using microfabricated electromagnets: experiments and simulations. *J. of Magnetism and Magnetic Materials* 293, 597-604.
- Smistrup, K., Bu, M. Q., Wolff, A., Bruus, H., Hansen, M. F., 2008, Theoretical analysis of a new, efficient microfluidic magnetic bead separator based on magnetic structures on multiple length scales. *Microfluidics and Nanofluidics* 4 (6), 565-573
- Smistrup, K., Lund-Olesen, T., Hansen, M. F., and Tang, P. T., 2006, Microfluidic magnetic separator using an array of soft magnetic elements. *J. Appl. Phys.* 99, 08P102-1-33.